

# Coupling Remote Sensing, Morphology, and Microclimate Simulation to Analyse Urban Heat in Mexico City, Mexico

[Author names and affiliations removed for blind review]

---

## Abstract

This paper proposes a city-to-street methodology to analyse urban heat in Mexico City by coupling remote sensing, urban morphology (Space Matrix), street network configuration (Space Syntax), and microclimate simulation (SOLWEIG/UMEP). At the macro scale, satellite-derived air temperature calibrated from Landsat 8/9 imagery (2014–2024) is overlaid with socio-demographic vulnerability indicators using Geographically Weighted Regression to identify thermo-social hotspots. Results show that 32% of blocks exceed the 26 °C health-risk threshold and 11% surpass 28 °C, concentrated in eastern boroughs where older adults, people with disabilities, and carless households co-locate with thermal hazard. At the meso scale, Space Matrix and Space Syntax metrics reveal that hotter zones are also more integrated: correlation between air temperature and NAIN strengthens from  $r = 0.105$  at 500 m to  $r = 0.285$  at 5 km. Ground Space Index emerges as the most influential morphological indicator ( $r = 0.228$  with Ta;  $r = -0.299$  with NDVI). At the micro scale, SOLWEIG simulations along highly integrated corridors show that mean radiant temperature (Tmrt)—not air temperature—governs pedestrian stress, with values exceeding 60 °C and PET above 41 °C. Three contributions emerge: (1) Tmrt as the appropriate indicator for pedestrian thermal load; (2) the spatial overlap of thermal exposure and social vulnerability; and (3) two mechanisms—structural heat in compact fabrics and corridor heat along integrated axes.

**Keywords:** Urban Heat Island, Space Syntax, Space Matrix, Mean Radiant Temperature, Mexico City

---

## 1. Introduction

Cities are experiencing rapid escalation of heat-related risks with measurable health, economic and urban consequences worldwide. In 2024, the planet recorded the warmest year since instrumental observations began. The Lancet Countdown 2024 reports record highs in heat-attributable mortality among those aged 65 and over and in productivity losses due to thermal exposure (?). The IPCC emphasises that cities concentrate exposure, vulnerabilities and agency, demanding explicitly urban policies and metrics.

Within this context, Mexico City is a critical case where intense urban heat intersects with social and spatial inequalities that amplify vulnerability. Three practical gaps motivate this research: identifying where exposure is concentrated and which vulnerable groups are most

affected; explaining which features of urban form and street network sustain these hotspots; and translating this understanding into verifiable passive design targets.

The study addresses three research questions:

- **Q1.** Where, and to what extent, do daytime summer air temperatures at block level co-locate with socially vulnerable groups under thresholds of 26 °C or more?
- **Q2.** Which combinations of urban form/density and network configuration best characterise thermal–social hotspots?
- **Q3.** In highly integrated, strongly exposed pedestrian corridors, how can micro-scale thermal stress be assessed to define passive design targets?

These questions form a logical chain: Q1 establishes *where* and *with whom* to intervene; Q2 clarifies *why* (form and network); Q3 specifies *how much* and *with what* to reduce heat.

## 2. Methodology

The methodology is structured across three nested spatial scales—macro, meso, and micro—from citywide screening to street-level simulation.

### 2.1. Macro Scale

Level-2 Landsat 8/9 summer imagery (1 June–30 August, 2014–2024) was processed in Google Earth Engine with radiometric corrections, NDVI, NDBI and shortwave albedo. Land surface temperature was empirically converted to air temperature using hourly RedMet observations from 18 stations ( $T_a = 0.5540 \times LST + 5.7606$ ), addressing the city's high-altitude and low-humidity conditions (?).

Socio-demographic indicators from the 2020 Mexican Census at block level captured vulnerable groups: aged 65+, children 6–14, people with disabilities, carless households, lack of health services, economic inactivity, and incomplete primary education. Geographically Weighted Regression (GWR) by borough identified blocks where thermal hazard ( $\geq 26^\circ\text{C}$ ;  $\geq 28^\circ\text{C}$ ) and social sensitivity statistically co-locate.

### 2.2. Meso Scale

Urban morphology was quantified through Space Matrix indicators: Floor Space Index (FSI), Ground Space Index (GSI), and Open Space Ratio (OSR) (?). A typological labelling classified blocks into categories including Dense Perimeter, Continuous Compact Low, Medium Perimeter, Low Perimeter, and Mixed forms.

The street network was modelled as a segment graph with Normalised Angular Integration (NAIN) and Normalised Angular Choice (NACH) computed at 500, 1,000, 1,500, and 5,000 m radii (?). Thermal attributes were sampled within 10-m buffers along segments and classified into hazard categories: Baseline ( $T_a < 26^\circ\text{C}$ ), Hazard 1 ( $26\text{--}28^\circ\text{C}$ ), and Hazard 2 ( $\geq 28^\circ\text{C}$ ).

### **2.3. Micro Scale**

Representative clusters with high thermal severity and high NAIN/NACH were simulated with UMEP/SOLWEIG in QGIS (?). High-resolution DEM/DSM (1 m), building footprints from Google Open Buildings, and NDVI-derived canopy layers provided inputs. Mean radiant temperature ( $T_{mrt}$ ), UTCI, and PET were computed at 10:00, 12:00, and 14:00 along observation points on highly integrated corridors in three cases: Hospital General, Airport, and Basílica de Guadalupe.

## **3. Results**

### **3.1. Macro Scale: Thermal–Social Hotspots**

The decadal climatology reveals average air temperatures reaching 26.8 °C in central and eastern boroughs (Cuauhtémoc, Iztacalco, Venustiano Carranza, Iztapalapa), versus 23–24 °C in peripheral vegetated areas (Xochimilco, Milpa Alta, Tlalpan). Approximately 32% of all blocks exceed the 26 °C health-risk threshold, while 11% surpass 28 °C during summer means.

The GWR analysis shows strong co-location between hotter blocks and socially sensitive groups. The share of older adults (65+) shows consistently positive associations, especially in Milpa Alta, Xochimilco and Tláhuac. Disability emerges as relevant in southern and eastern boroughs. Car absence becomes significant in peripheral zones where long public transport commutes intensify heat exposure.

The eastern boroughs—Iztapalapa, Tláhuac, and Gustavo A. Madero—accumulate the highest coefficients across multiple variables (Figure 1).

### **3.2. Meso Scale: Form–Network Coupling**

Across all radii, hotter areas (Hazard 2) displayed the highest NAIN and NACH values. At 5 km, NAIN reached 1.31 in Hazard 2 versus 0.82 in Hazard 0. The correlation between  $T_a$  and NAIN strengthened with radius—from  $r = 0.105$  at 500 m to  $r = 0.285$  at 5 km—indicating that the city’s hottest areas occupy structurally advantaged positions in the metropolitan network.

Ground Space Index (GSI) emerged as the most influential morphological indicator, negatively correlated with NDVI ( $r = -0.299$ ) and positively with  $T_a$  ( $r = 0.228$ ). Dense Perimeter and Continuous Compact Low typologies registered the highest Heat Index values (1.214 and 1.188), combining compact built form with limited open space (Figure 2).

Two reinforcing mechanisms emerge: *structural heat* in compact, sealed fabrics where higher GSI correlates with lower vegetation; and *corridor heat* along highly integrated axes where least-angle pedestrian spines combine flows and exposure.

### **3.3. Micro Scale: Biometeorological Simulations**

The three cases reveal a progressive gradient of vulnerability. In Case 1 (Hospital General), vulnerability is anchored in moderate heat (26–28 °C), with UTCI rising from 29.6 °C at 10:00 to 32.9 °C at 14:00 (strong stress), while  $T_{mrt}$  climbed from 42.7 °C to 55.0 °C. In Case 2 (Airport),

Hotspots térmico-sociales (GWR) — Umbrales fijos  
gris: sin hotspot · naranja: 26-<28 °C · rojo:  $\geq 28$  °C

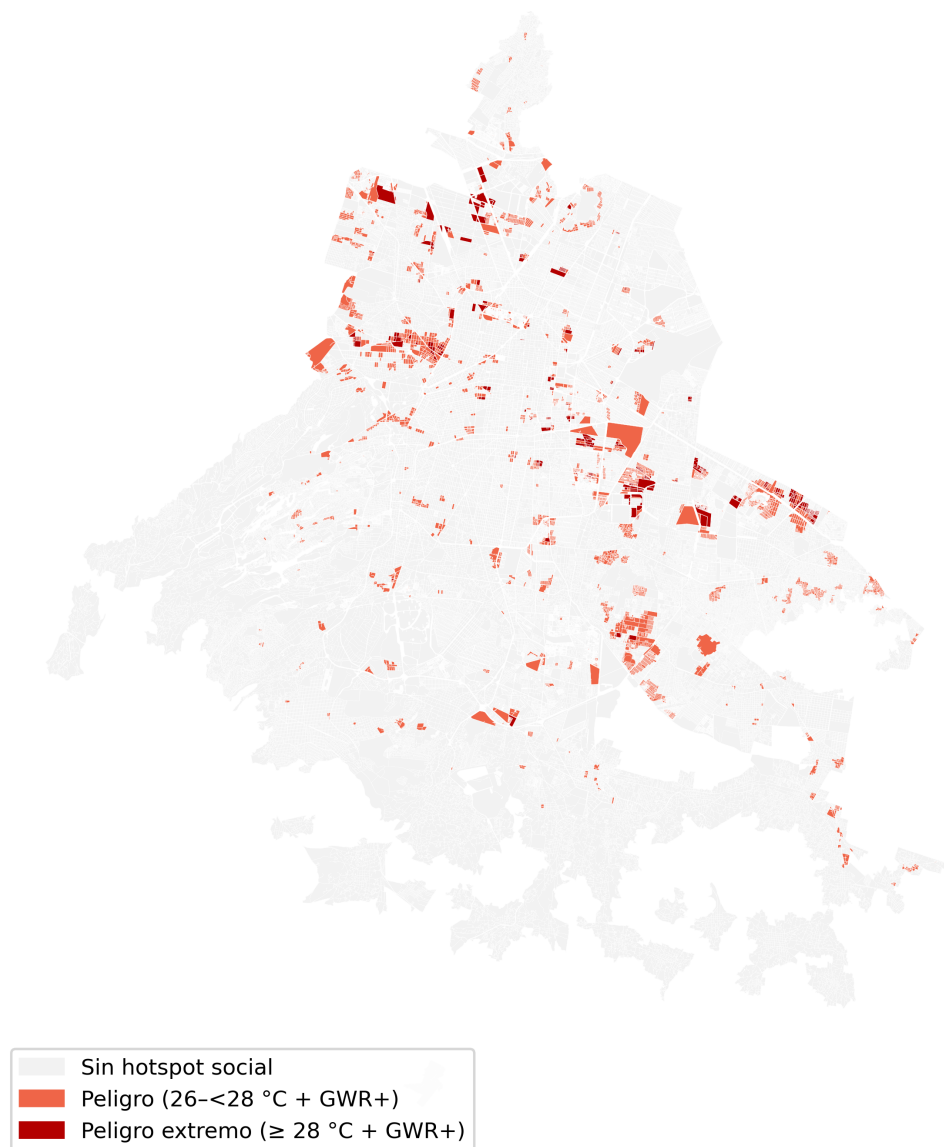


**Figure 1:** Thermo-social hotspots. Red areas indicate blocks where thermal hazard ( $\geq 26$  °C or  $\geq 28$  °C) co-locates with statistically significant social vulnerability.

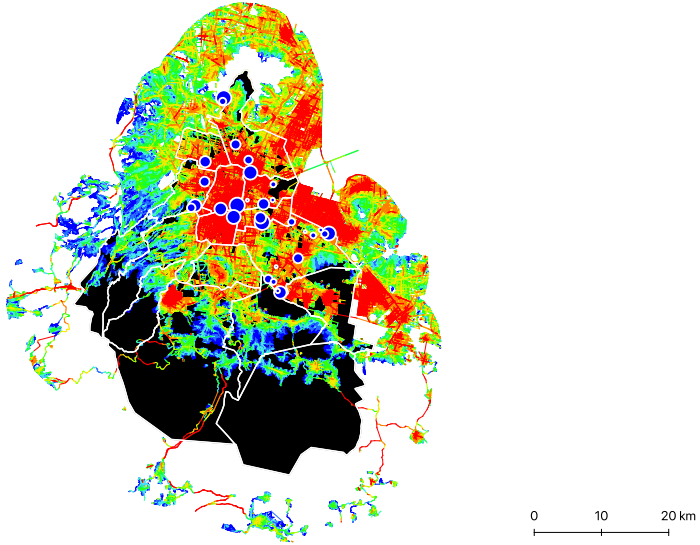


**Figure 2:** Normalised Angular Integration (NAIN) at  $r = 1,500\text{ m}$ . Warmer colours indicate higher integration, which correlates with thermal hazard.

UTCI held steady at 34–35°C and Tmrt exceeded 63°C. In Case 3 (Basílica), vulnerability emerges at  $\geq 28^\circ\text{C}$ , with PET reaching 41.5°C and Tmrt peaking at 65.8°C (Figure 3).

Blocks with Ta in the 26–28°C band still produced Tmrt above 60°C and PET above 41°C, demonstrating why Ta alone understates street-level risk. The hottest patches consistently coincided with high-integration corridors.

#### 4. Conclusions

This research demonstrates a city-to-street pipeline for analysing urban heat. Three findings stand out:

1. **Tmrt governs pedestrian heat stress.** Under Mexico City's high-irradiance, dry-air conditions, mean radiant temperature—not LST or Ta—determines thermal load at midday. Design targets should be formulated against biometeorological rather than surface metrics.
2. **Exposure is unequal and socially structured.** Strong co-location exists between hotter blocks and socially sensitive groups (older adults, people with disabilities, carless households), with borough-heterogeneous associations.
3. **Two mechanisms translate morphology and networks into lived heat.** Structural heat arises in compact, sealed fabrics (high GSI, low NDVI), while corridor heat emerges along highly integrated axes.

The policy implication is that heat adaptation should be reframed around measurable outcomes. Suitable KPIs could include median midday Tmrt reductions of 10–15°C along priority



**Figure 3:** Mean radiant temperature ( $T_{mrt}$ ) at 14:00 in Case 1 (Hospital General). High-integration corridors experience the highest radiative loads.

corridors, continuous shade over at least 70% of pedestrian length between 10:00 and 14:00, and cooling refuges every 300–500 m. Passive cooling—shade, ventilation and non-glare cool materials—reduces cooling demand, avoiding energy poverty while protecting those least able to afford mechanical cooling.

The contribution is twofold: substantively, the research demonstrates that thermal justice is a spatial reality; methodologically, it advances a replicable framework linking metropolitan screening to micro-climatic simulation using open tools (Google Earth Engine, DepthmapX, UMEP/QGIS).

## References

- Berghauer Pont, M. and Haupt, P. (2020) *Spacematrix: Space, Density and Urban Form*. 2nd ed. Rotterdam: nai010 publishers.
- Chakraborty, T. et al. (2022) ‘Lower urban humidity moderates outdoor heat stress’, *AGU Advances*, 3(4), e2022AV000729.
- Hillier, B. and Hanson, J. (1984) *The Social Logic of Space*. Cambridge: Cambridge University Press.
- Hillier, B., Yang, T. and Turner, A. (2012) ‘Normalising least angle choice in Depthmap’, *Journal of Space Syntax*, 3(2), pp. 155–193.
- INEGI (2021) *Censo de Población y Vivienda 2020*. Aguascalientes: Instituto Nacional de Estadística y Geografía.
- Lindberg, F., Holmer, B. and Thorsson, S. (2008) ‘SOLWEIG 1.0—Modelling spatial variations of 3D radiant fluxes and mean radiant temperature’, *International Journal of Biometeorology*, 52, pp. 697–713.
- Magaña, V. and Vargas, M. (2020) ‘Umbrales de temperatura para la salud en México’, *Salud Pública de México*, 62(4), pp. 389–391.
- Romanello, M. et al. (2024) ‘The 2024 report of the Lancet Countdown on health and climate change’,

*The Lancet*, 404, pp. 1–55.